PERGAMON

International Journal of Solids and Structures 40 (2003) 4135–4151

INTERNATIONAL JOURNAL OF SOLIDS and STRUCTURES

www.elsevier.com/locate/ijsolstr

Finite displacement static analysis of thin plate with an opening—a variational approach

A.V. Singh *, U.K. Paul

Department of Mechanical and Materials Engineering, The University of Western Ontario, London, Ont., Canada N6A 5B9

Received 24 March 2003

Abstract

A generalized work–energy method for the linear and geometrically nonlinear static analysis of thin isotropic plate with a cutout is presented. The plate geometry is divided into few quadrilateral segments. Each segment is defined by four curved edges and the natural coordinates in conjunction with the Cartesian coordinates are used in formulating the stiffness matrix and the load vector. Two different sets of interpolating functions are used for the geometric and displacement representations respectively. The matrix equation of equilibrium is derived from the variational principle. By exploiting the geometric symmetry, numerical results are obtained for the following examples: (a) square plate with circular opening at the centre and (b) circular plate with circular or square inner boundary. The plates are subjected to uniformly distributed load and both the pinned and fixed outside boundary conditions are considered. Very good comparison is observed between the present results and those published in the literature for the fixed square plate without an opening. Effects of the opening size on the displacement are examined in detail.

Keywords: Finite deformation; Nonlinear plate theory; First order shear deformable plate; Ritz method

1. Introduction

Courant (1943) presented a general view of the mathematicians, physicists and engineers towards the variational methods for the solution of equilibrium and vibration problems. According to Courant, the energy method was envisaged independently by Lord Rayleigh and W. Ritz for the numerical solutions of vibration problems. Lord Rayleigh, in his book—Theory of Sound (vol. 1, 1877 and vol. 2, 1896) and in other publications, was the first to use this method. In his publications in 1908 and 1909, Ritz gave masterly account of the energy method and applied it to the plate vibration problem. Courant also raised some minor objections to the Rayleigh–Ritz method, which were related more to the computational tools available in those days and time than the method itself. In a review paper, Higgins (1943) described the work of Ritz who used variational method to solve torsion problem. In the following, works of some

* Corresponding author. Tel.: +1-519-661-2111; fax: +1-519-661-3020.
E-mail address: avsingh@eng.uwo.ca (A.V. Singh).

0020-7683/03/$ - see front matter © 2003 Elsevier Science Ltd. All rights reserved.
doi:10.1016/S0020-7683(03)00204-X

Nomenclature

a	reference length parameter used for normalization
E, ν	modulus of elasticity and Poisson's ratio
h	plate thickness
k	shear correction factor
$[k_L]$, $[k_{NL}]$	linear and nonlinear stiffness matrices
$N_j(\xi,\eta)$	geometric shape function
p	load per unit area
pa^4/Eh^4	dimensionless load parameter
U	strain energy
W	work by mechanical forces
u, v, w	displacement components at the reference plane of the plate
x, y, z	Cartesian coordinates
β_1, β_2	components of rotation of the normal to the middle plane
ε_x, ε_y	linear strain components at the middle plane
γ_{xy}, γ_{yz}, γ_{zx}	linear shear strains at the middle plane
κ_x, κ_y, κ_{xy}	linear curvature-like terms
$\{\Gamma\}^T$	$\{U_1 \quad V_1 \quad W_1 \quad \Phi_1 \quad \Theta_1 \quad \cdots\}$
ϕ_x, ϕ_y, ϕ_{xy}	nonlinear strain components
$\{\Delta\}^T$	$\{u \quad v \quad w \quad \beta_1 \quad \beta_2\}$, displacement vector
$\{\chi\}^T$	$\{\varepsilon_x \quad \varepsilon_y \quad \gamma_{xy} \quad \gamma_{yz} \quad \gamma_{zx} \quad \kappa_x \quad \kappa_y \quad \kappa_{xy}\}$, strain-curvature vector
Ω_L, Ω_{NL}	linear and nonlinear energy functionals
$\psi_j(\xi,\eta)$	displacement shape function
ξ, η	parametric coordinates for mapping the geometry

distinguished researchers who used Rayleigh–Ritz (or related) method to solve static and vibration problems are briefly discussed first. Then, some description of the work done on the geometrically nonlinear (GNL) analysis of thin elastic plates by other researchers is also presented.

By applying the energy method and simple algebraic polynomial that satisfied the slope and deflection boundary conditions, Pickett (1939) obtained the static deflections and moments due to lateral load on a clamped rectangular plate. He concluded that the method worked better for the uniformly distributed load than the point load. In his paper Pickett also mentioned that the energy method was developed by Timoshenko (1934) and Ritz. Young (1950) published his work on the vibration of rectangular plates by the Ritz method. According to him, there were little published data for the vibration of rectangular plates by Ritz method except for the completely free square plate, which was investigated by Ritz himself. Using the functions defining the normal modes of vibration of a uniform beam, Young obtained results for the frequencies and associated mode shapes for three specific problems: (i) square cantilever plate, (ii) square plate clamped at all sides and (iii) square plate having two adjacent sides clamped and other two edges free. Warburton (1954), using the Rayleigh method and assuming that waveforms of vibrating plates and beams are similar, derived approximate frequency formulas for 21 combinations of boundary conditions.

Leissa (1969) published a monograph which inspired literally hundreds of researchers and tremendous amount of interest was shown on the topic of vibration of plates. He then published a paper (Leissa, 1973) giving comprehensive and accurate results for the free vibration of rectangular plates. Exact characteristic equations were derived for six cases having two opposite sides simply supported and other two with various combinations of clamped, simply supported and free edges. He then went on to study 15 other cases,

without the two opposite sides simply supported, using the Rayleigh–Ritz method with beam functions. For the next three decades, Leissa applied Rayleigh–Ritz method with great success using algebraic polynomials to many plate, shell and solid problems. From then on, many researchers used this method in the field of plate and shell vibrations.

In this paper, the authors present a numerical procedure based on the work–energy method (a modified form of the Ritz method) for the static analysis of geometrically nonlinear thin elastic plates. Levy (1942a,b) solved the *Th. von Karman's* nonlinear differential equation for the analysis of rectangular plates with conditions: (a) simply supported on four sides (NACA TR 737) and (b) fully clamped plate under normal pressure (NACA TR 740). Results from Levy's study became the standard and are used even today by researchers working on this problem. Wang (1948) solved *von Karman's* equations numerically for the simply supported rectangular plates having aspect ratios 1.5 and 2.0. Approximate solutions and the comparison of results with exact solutions in the literature for the large deflections of rectangular and circular plates with uniformly distributed load were reported by Berger (1955). An excellent bibliography, enlisting more than 400 journal papers on nonlinear static analysis of circular, rectangular and other shaped plates, is given in the book by Satyamoorthy (1997). Majority of the papers deals with the problem solved through classical methods. The geometrically nonlinear analysis of rectangular plates received significant attention from researchers working with the finite element methods. Murray and Wilson (1969) studied large deflection behaviour of simply supported square plates and plates undergoing cylindrical bending. Yang (1972) analysed rectangular plates using the matrix incremental method and successfully compared deflections and stresses with the results of Levy (1942a,b). A nonlinear quadrilateral plate-bending-element procedure based on the von Karman strain expressions and Marguerre shallow shell theory was applied by Bergan and Clough (1973) to study the stability and large deflection characteristics of plates and shallow shells. Pica et al. (1980) presented a geometrically nonlinear finite element formulation for the bending of first order shear deformable plates under the assumption of small rotations and reported numerical results for square, skew, circular and elliptical plates. Singh and Elaghabash (2003) studied the large static deflection analysis of square and rhombic plates using the Ritz method. They compared deflection and stresses with the results of Levy (1942a,b), Rushton (1970), Pica et al. (1980) and ANSYS.

In this work, the plate geometry is divided into quadrilateral segments, each of which is bounded by four curved/straight edges. Further, the segments are mapped into square using the natural coordinates so that mathematics in the procedure becomes simple and straightforward. A segment is defined in the Cartesian coordinate system using eight geometric nodes, four located at the corner points and the other four at the mid-points of the four edges respectively. Plate equations are based on the first order shear deformation theory known as the "*Reissner–Mindlin plate theory*". The nonlinearity is associated with the in-plane strain components only and the form of the transverse shear strain components and the curvature like terms remains linear. The displacement fields are defined by much higher order shape functions than the ones used for the geometric nodes and are associated with the prescribed displacement nodes on boundary and inside of the plate segment. The model, generally, consists of only a few segments and the components of displacement and rotation of the normal to the plate surface are matched when the displacement nodes are located on an edge shared by two segments. The boundary conditions are applied at the displacement nodes. Considered in this study as numerical examples are the uniformly loaded plate of types: (a) rectangular plate with a circular hole at the geometric centre, (b) circular annular plate, and (c) circular plate with a square opening. The geometric symmetry is used in all calculations.

2. Definition of a plate quadrilateral

In order to create a model for the analysis the middle surface area of plate is divided into a number of quadrilateral segments, each of which is bounded by four edges in the x–y plane as shown in Fig. 1. The

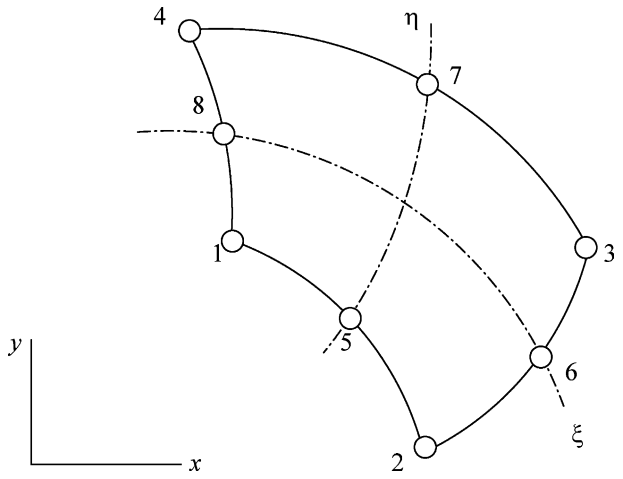

Fig. 1. A typical plate segment with geometric nodes.

plate thickness (h) is assumed to be small in comparison with the other dimensions in the x–y plane. The four corner points are denoted by numbers 1–4 in a counter clockwise sense and the middle edge points by 5–8 as shown. Indices x, y and z represent the coordinates at an arbitrary point in the plate, where z is measured from the middle plane. Coordinates of the geometric nodes are expressed by (x_j, y_j) with $j = 1, 2, 3, \ldots, 8$. The procedure developed in this study makes use of the parametric coordinates ξ and η which map the quadrangle into a square bounded by $-1 \leqslant (\xi \text{ or } \eta) \leqslant +1$. The coordinates of an arbitrary point are interpolated by the following:

$$\begin{aligned} x(\xi,\eta) &= \sum_{j=1}^{8} N_j(\xi,\eta) x_j \\ y(\xi,\eta) &= \sum_{j=1}^{8} N_j(\xi,\eta) y_j \end{aligned} \tag{1}$$

Here, $N_j(\xi,\eta)$ for $j = 1, 2, 3, \ldots, 8$ are known as the shape functions (Weaver and Johnston, 1984). From here on, all functionals of the plate are expressed in terms of the parametric coordinates ξ and η. The Jacobian matrix $[J(\xi,\eta)]$ and its determinant $|J(\xi,\eta)|$ are used in the derivation of the plate equations.

3. Nonlinear elastic plate equations

The displacement components along the Cartesian axes at a point in the plate are denoted by u', v' and w'. Furthermore, the displacement components customarily are expressed in terms of their counter parts at the middle plane of the plate:

$$\begin{aligned} u' &= u + z\beta_1 \\ v' &= v + z\beta_2 \\ w' &= w \end{aligned} \tag{2}$$

In the above, all terms on the right hand side are referred from the middle plane of the plate. Symbols u, v, w denote the displacement components; β_1 and β_2 are the components of the rotation of the normal to the

middle plane of the plate; z is the distance measured from the reference plane in the direction perpendicular to the plate.

The method requires work–energy expressions for the derivation of the matrix equation of equilibrium. To proceed in that direction, some vectors containing strains and curvatures as the components are introduced for convenience. These are:

$$\begin{aligned}
\{\Delta\}^{\mathrm{T}} &= \{\, u \quad v \quad w \quad \beta_1 \quad \beta_2 \,\} \\
\{\chi_{\mathrm{L}}\}^{\mathrm{T}} &= \{\, \varepsilon_x \quad \varepsilon_y \quad \gamma_{xy} \quad \gamma_{yz} \quad \gamma_{zx} \quad \kappa_x \quad \kappa_y \quad \kappa_{xy} \,\} \\
\{\chi_{\mathrm{NL}}\}^{\mathrm{T}} &= \{\, \varepsilon_x \quad \varepsilon_y \quad \gamma_{xy} \quad \phi_x \quad \phi_y \quad \phi_{xy} \,\}
\end{aligned} \tag{3}$$

Subscripts L and NL stand for linear and nonlinear cases respectively. The details of the various components are defined in terms of the displacement and rotation components:

$$\begin{aligned}
&\varepsilon_x = \frac{\partial u}{\partial x} \qquad \varepsilon_y = \frac{\partial v}{\partial y} \\
&\gamma_{xy} = \frac{\partial u}{\partial y} + \frac{\partial v}{\partial x} \qquad \gamma_{yz} = \frac{\partial w}{\partial y} + \beta_2 \\
&\gamma_{zx} = \frac{\partial w}{\partial x} + \beta_1 \\
&\kappa_x = \frac{\partial \beta_1}{\partial x} \qquad \kappa_y = \frac{\partial \beta_2}{\partial y} \qquad \kappa_{xy} = \frac{\partial \beta_1}{\partial y} + \frac{\partial \beta_2}{\partial x} \\
&\phi_x = (1/2)\left(\frac{\partial w}{\partial x}\right)^2 \qquad \phi_y = (1/2)\left(\frac{\partial w}{\partial y}\right)^2 \qquad \phi_{xy} = \frac{\partial w}{\partial x}\frac{\partial w}{\partial y}
\end{aligned} \tag{4}$$

Eq. (4) is based on the nonlinear elastic strain–displacement relationships given by Novozhilov (1953). Using Eq. (4), and the stress–strain relationships (Singh and Elaghabash, 2003), we can derive the following form for the strain energy in terms of displacement components including components for the rotation of the normal to the plate and elastic material properties:

$$U = (1/2)\int_{-1}^{+1}\int_{-1}^{+1} (\Omega_{\mathrm{L}} + \Omega_{\mathrm{NL}})|J(\xi,\eta)|\,\mathrm{d}\xi\,\mathrm{d}\eta \tag{5}$$

where

$$\Omega_{\mathrm{L}} = \{\chi_{\mathrm{L}}\}^{\mathrm{T}}[D]\{\chi_{\mathrm{L}}\} \quad \text{and} \quad \Omega_{\mathrm{NL}} = \{\chi_{\mathrm{NL}}\}^{\mathrm{T}}[\overline{D}]\{\chi_{\mathrm{NL}}\} \tag{6}$$

Vector $\{\chi_{\mathrm{L}}\}$ contains midplane linear strain and curvature terms. Similarly, $\{\chi_{\mathrm{NL}}\}$ is made of membrane strain components containing both linear and nonlinear terms. Matrices $[D]_{8\times 8}$ and $[\overline{D}]_{6\times 6}$ are symmetric with majority of the components being zero. Their non-zero terms are given below:

$$\begin{aligned}
&D_{11} = D_{22} = \overline{D}_{14} = \overline{D}_{41} = \overline{D}_{44} = \overline{D}_{25} = \overline{D}_{52} = \overline{D}_{55} = K_0 \\
&D_{12} = D_{21} = \overline{D}_{24} = \overline{D}_{42} = \overline{D}_{15} = \overline{D}_{51} = \overline{D}_{45} = \overline{D}_{54} = vK_0 \\
&D_{33} = \overline{D}_{36} = \overline{D}_{63} = \overline{D}_{66} = 0.5(1-v)K_0; \quad D_{44} = D_{55} = kD_{33} \\
&D_{66} = D_{77} = D_0; \quad D_{67} = D_{76} = vD_0; \quad D_{88} = 0.5(1-v)D_0 \\
&K_0 = E\bar{h}/(1-v^2); \quad D_0 = (1/12)E\bar{h}^3/(1-v^2)
\end{aligned} \tag{7}$$

The parameter k is the shear correction factor in the above equation and its value is (5/6). Since the integration over the plate thickness has already been performed, only the integration of the area of the middle plane remains to be carried over.

4. Displacement fields, stiffness matrix and load vector for the quadrilateral

In this section, we discuss the procedure for generating the stiffness matrix and the load vector for the plate quadrilateral defined earlier in Section 2. The interpolating functions for the displacement fields are of much higher order than that for the geometry. Therefore, it is now necessary to introduce a different set of nodes, which may be termed as the displacement nodes. Shown in Fig. 2 is a 7×6 grid of 42 points to which displacement degrees of freedom are assigned. To be consistent with the grid size shown in Fig. 2, we consider fifth order polynomial in ξ and a sixth order polynomial in η as interpolating functions. Each point in this figure is assigned five degrees of freedom, such as $(U_j \quad V_j \quad W_j \quad \Phi_j \quad \Theta_j)$ corresponding to u, v, w and β_1 and β_2 respectively at the jth node. It is now simple to write the components of displacement and the rotation of the normal as given below:

$$
\begin{aligned}
u &= \sum_{j=1}^{n} U_j \psi_j(\xi,\eta) \\
v &= \sum_{j=1}^{n} V_j \psi_j(\xi,\eta) \\
w &= \sum_{j=1}^{n} W_j \psi_j(\xi,\eta) \\
\beta_1 &= \sum_{j=1}^{n} \Phi_j \psi_j(\xi,\eta) \\
\beta_2 &= \sum_{j=1}^{n} \Theta_j \psi_j(\xi,\eta)
\end{aligned}
\tag{8}
$$

The interpolating functions $\psi_j(\xi,\eta)$ in Eq. (8) can be deduced in the same manner as $N_j(\xi,\eta)$ in Eq. (1). In the present formulation, eight nodal points are used for the geometry definition, whereas $n = (p+1)(q+1)$

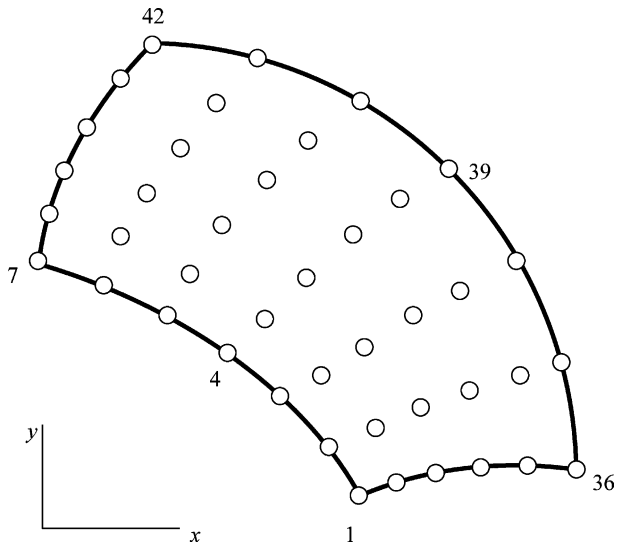

Fig. 2. The displacement nodes for a plate segment.

displacement nodes are used. Indices p and q denote respectively the orders of the polynomials in ξ and η. The matrix form of the above equation is

$$\{\Delta\} = [\,[\psi_1(\xi,\eta)] \quad [\psi_2(\xi,\eta)] \quad [\psi_3(\xi,\eta)] \quad [-] \quad [-] \quad [\psi_n(\xi,\eta)]\,]\{\Gamma\} \tag{9}$$

where $\{\Gamma\}^{\mathrm{T}} = \{\, U_1 \quad V_1 \quad W_1 \quad \Phi_1 \quad \Theta_1 \quad U_2 \quad V_2 \quad W_2 \quad \Phi_2 \quad \Theta_2 \quad U_3 \quad V_3 \quad \cdots \}$ and contains the displacement and rotation components for each displacement node. Matrix $[\psi_j(\xi,\eta)]_{5\times 5}$ corresponds to the jth displacement node and is given below:

$$[\psi_j(\xi,\eta)] = \begin{bmatrix} \psi_j(\xi,\eta) & 0 & 0 & 0 & 0 \\ 0 & \psi_j(\xi,\eta) & 0 & 0 & 0 \\ 0 & 0 & \psi_j(\xi,\eta) & 0 & 0 \\ 0 & 0 & 0 & \psi_j(\xi,\eta) & 0 \\ 0 & 0 & 0 & 0 & \psi_j(\xi,\eta) \end{bmatrix} \tag{10}$$

By substituting Eq. (9) into Eq. (4) and using the vectors $\{\chi_{\mathrm{L}}\}$ and $\{\chi_{\mathrm{NL}}\}$ introduced in (3), we get

$$\begin{aligned} \{\chi_{\mathrm{L}}\} &= [B_{\mathrm{L}}]\{\Gamma\} \\ \{\chi_{\mathrm{NL}}\} &= [B_{\mathrm{NL}}]\{\Gamma\} \end{aligned} \tag{11}$$

Because of the large size, matrices $[B_{\mathrm{L}}]_{8\times n}$ and $[B_{\mathrm{NL}}]_{5\times n}$ are not displayed in this paper. Substituting Eq. (11) into (5), we obtain the following strain energy expression in terms of the linear and nonlinear stiffness matrices:

$$U = (1/2)\{\Gamma\}^{\mathrm{T}}([k_{\mathrm{L}}] + [k_{\mathrm{NL}}])\{\Gamma\} \tag{12}$$

where

$$\begin{aligned} [k_{\mathrm{L}}] &= \int_{-1}^{+1}\int_{-1}^{+1} [B_{\mathrm{L}}]^{\mathrm{T}}[D][B_{\mathrm{L}}]|J(\xi,\eta)|\,\mathrm{d}\xi\,\mathrm{d}\eta \quad \text{and} \\ [k_{\mathrm{NL}}] &= \int_{-1}^{+1}\int_{-1}^{+1} [B_{\mathrm{NL}}]^{\mathrm{T}}[\overline{D}][B_{\mathrm{NL}}]|J(\xi,\eta)|\,\mathrm{d}\xi\,\mathrm{d}\eta \end{aligned} \tag{13}$$

Integration here can be carried out numerically using the Gaussian quadrature for which the number of integration points will depend upon the order of the polynomial used in the displacement fields.

The work done by a uniformly distributed load p_0 applied in the transverse direction of the plate under the assumed displacement field is

$$W = \int\int p_0 w\,\mathrm{d}x\,\mathrm{d}y \tag{14}$$

Substituting w from Eq. (8) into the above,

$$W = \int_{-1}^{+1}\int_{-1}^{+1} p_0 \sum_{j=1}^{n} W_j\psi_j(\xi,\eta)|J(\xi,\eta)|\,\mathrm{d}\xi\,\mathrm{d}\eta = \{\Gamma\}^{\mathrm{T}}\{p\} \tag{15}$$

In Eq. (15), $\{\Gamma\}$ is the displacement vector introduced in Eq. (9). The load vector consistent with the present formulation procedure is

$$\{p\}^{\mathrm{T}} = \{\, 0 \quad 0 \quad p_1 \quad 0 \quad 0 \quad \cdots \quad 0 \quad 0 \quad p_n \quad 0 \quad 0 \,\} \tag{16}$$

and $p_j = p_0 \int_{-1}^{+1}\int_{-1}^{+1} \psi_j(\xi,\eta)|J(\xi,\eta)|\,\mathrm{d}\xi\,\mathrm{d}\eta$. This load is applied in the transverse direction at each displacement node of the plate segment. Other components of the load vector are set to zero as shown in Eq. (16).

With the stiffness matrix and load vector defined above, we now work towards the derivation of the equilibrium equation with the help of the potential energy $\Pi = U - W$. The strain energy expression and work done by the applied load are both functions of the unknown terms of the displacement vector $\{\Gamma\}$. Using the minimum potential energy condition at the stable equilibrium of the plate, i.e. $\delta\Pi = 0$, we obtain equilibrium equation in the following form:

$$\begin{aligned} &\{\delta\Gamma\}^{\mathrm{T}}([k]\{\Gamma\} - \{\bar{p}\}) = 0 \quad \text{or} \\ &[k]\{\Gamma\} = \{\bar{p}\} \end{aligned} \tag{17}$$

In the above, $[k] = [k_{\mathrm{L}}] + [k_{\mathrm{NL}}]$. It should be kept under notice that the nonlinear part of the stiffness matrix $[k]$ is dependent upon the deformed configuration of the plate.

5. Numerical results and discussions

An energy method is developed in this paper for the analysis of plates with internal and external boundaries. The dimensionless transverse deflection (w/h) is calculated by varying the uniformly distributed transverse load normalized by $(Q = pa^4/Eh^4)$. The models selected for the analysis are: rectangular plate with a circular opening at the geometric centre, annular circular plate and circular plate with square opening at the centre. Because of the symmetry with regards to the geometry, load and the boundary conditions, only one quarter of the plate is analysed by enforcing the following conditions:

$$\begin{aligned} &v = \beta_2 = 0 \text{ on the } x\text{-axis} \\ &u = \beta_1 = 0 \text{ on the } y\text{-axis} \end{aligned} \tag{18}$$

Case 1. Rectangular plate with a circular opening. Shown in Fig. 3 is the quarter model of a rectangular plate having its length and width as (a) and (b) respectively. This plate also has a circular opening of diameter (d) at the geometric centre and the load considered is uniformly distributed over the surface area. The symmetry conditions given in Eq. (18) are used on edges AB and ED respectively. The quarter plate model is further subdivided into four segments identified by Roman numerals I–IV in Fig. 3.

In the present scheme, which can also be termed as the sub-parametric finite element formulation, two types of grid points are introduced. The first type includes eight geometric nodes, which are located at the

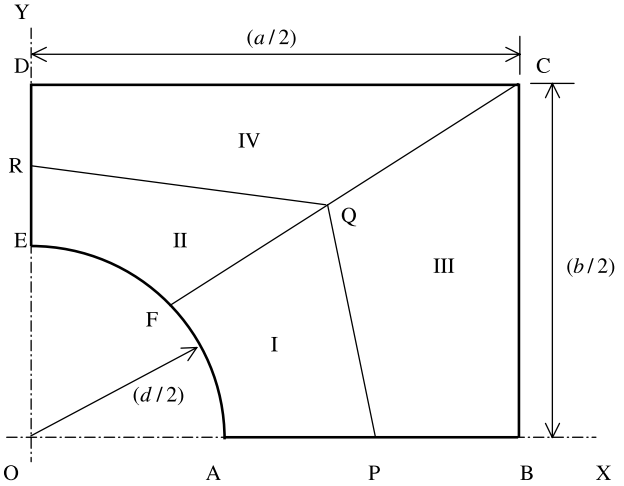

Fig. 3. Quarter of a rectangular plate with circular opening.

four corners and mid points of the four edges of each segment (Fig. 1). The second type includes the displacement grids (or nodes), the number of which depends upon polynomial orders used in generating the displacement field functions (Fig. 2). In the present analysis, fourth order polynomials in both ξ and η directions are used for each segment and therefore, the grid size for each segment is 5×5 with 25 points.

The model is also assigned grid points with global significance. Since fourth order interpolation functions are used in both ξ and η directions, there are nine nodes on each of APB, BCD, DRE, EFA, PQR and FQC. In all, there are $9 \times 9 = 81$ displacement grid points, each having five degrees of freedom corresponding to u, v, w, β_1 and β_2. The size of the stiffness matrix and load vector for each segment is $25 \times 5 = 125$. The same for the entire model is $81 \times 5 = 405$. Numerical results are obtained for the cases identified by the following boundary conditions. The stiffness matrices for all of four segments are computed separately and then assembled to obtain the overall stiffness matrix for the entire model. Similarly, the load vector is generated for each segment and then assembled as a global load vector. The nonlinear equation of equilibrium (17) is solved iteratively (Singh and Elaghabash, 2003). The thickness to length ratio (h/a) used in all the calculations is 0.01.

(i) Outside boundary pinned and inside free. For this case, the outside boundary BCD is subjected to:

$$\begin{aligned} &u = v = w = 0 \text{ on BC and CD,} \quad \text{and} \\ &\text{no condition on the inside boundary EFA.} \end{aligned} \tag{19}$$

(ii) Outside boundary pinned and inside edge constrained in the plane of the plate. The displacement boundary conditions used for this case are:

$$\begin{aligned} &u = v = w = 0 \text{ on BC and CD,} \quad \text{and} \\ &u = v = \beta_1 = \beta_2 = 0 \text{ on the inside boundary EFA.} \end{aligned} \tag{20}$$

(iii) Outside boundary fixed and inside free. For this case, the outside boundary BCD is subjected to the following:

$$\begin{aligned} &u = v = w = \beta_1 = \beta_2 = 0 \quad \text{and} \\ &\text{no condition on EFA.} \end{aligned} \tag{21}$$

(iv) Outside boundary fixed and inside edge constrained in the plane of the plate. For this case, the boundary conditions used are:

$$\begin{aligned} &u = v = w = \beta_1 = \beta_2 = 0 \text{ on the edge BCD} \quad \text{and} \\ &u = v = \beta_1 = \beta_2 = 0 \text{ on the edge EFA.} \end{aligned} \tag{22}$$

Figs. 4 and 5 show the other two models each having outside circular boundary. Fig. 6 shows the load ($Q = pa^4/Eh^4$) versus deflection (w/h) curves corresponding to case (i) for $d/a = 0.0$, 0.1, 0.2, 0.3 and 0.4. For the case of the free opening, deflection results corresponding to $d/a > 0.4$ are not reported here because of the convergence problem. Simply results do not converge if $d/a > 0.4$ and $Q > 200$. This convergence problem does not appear when the inside boundary is constrained in the plane of the plate. Results for this case are presented in Fig. 7 for $d/a = 0.0$, 0.1, 0.2, 0.3, 0.4 and 0.5. Deflections increase with the load and are seen to vary monotonically. Results converge rapidly in only a few iterations for the lower load levels, but the convergence rate deteriorates when both the load (Q) and hole diameter index (d/a) increase. The deflection at the edge of the hole is lower for higher values of (d/a). As expected, the plate deflection due to a given load in Fig. 7 is lower than the corresponding case shown in Fig. 6 with no conditions at the circular opening. The effect of the hole size is very small for the case in which no condition is applied at it. But this effect becomes quite significant, if the inside boundary is restrained from in-plane movement. Calculations

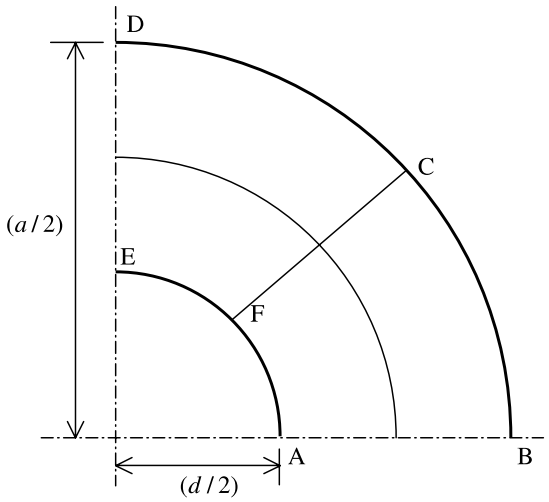

Fig. 4. Quarter of an annular circular plate.

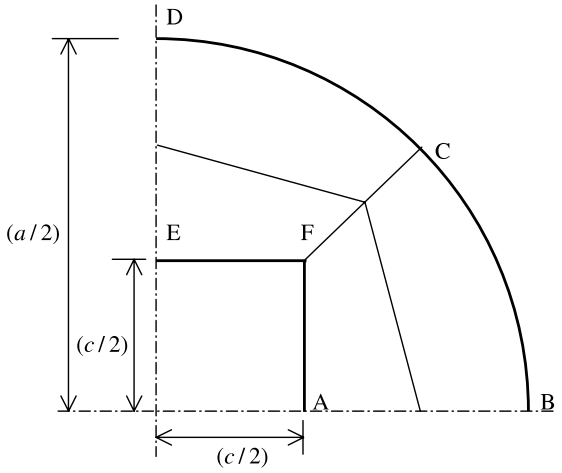

Fig. 5. Quarter of a circular plate with square opening.

are done for the zero diameter hole with and without constraints and the results are plotted in Figs. 6 and 7 using symbol (o). In both cases, the values are very close to each other. Results are also obtained for the rectangular plates as shown in Fig. 8 for aspect ratios of $b/a = 0.5$, 0.6, 0.7, 0.8, 0.9 and 1.0. The load/deflection curve shows similar pattern as that for the square plate and for the same load the deflections (w/h) increase with the increasing values of (b/a). Numerical results for the fixed square plate with $d/a = 0.0$, 0.1, 0.2, 0.3, 0.4 and 0.5 are shown in Figs. 9 and 10 for cases (iii) and (iv) respectively. After examining Figs. 6 and 9, where no condition is applied at the inside boundary, it is seen that the hole diameter has very little effect on the deflection of the plate if the outside boundary is pinned and has considerable influence if the outside boundary is fixed. The influence of the hole diameter is significantly higher when the inside edge is constrained, as seen in Fig. 10. The present results for $d/a = 0$ in Figs. 9 and 10 show very good agreement with previously published data by Levy (1942b) for the full square plate.

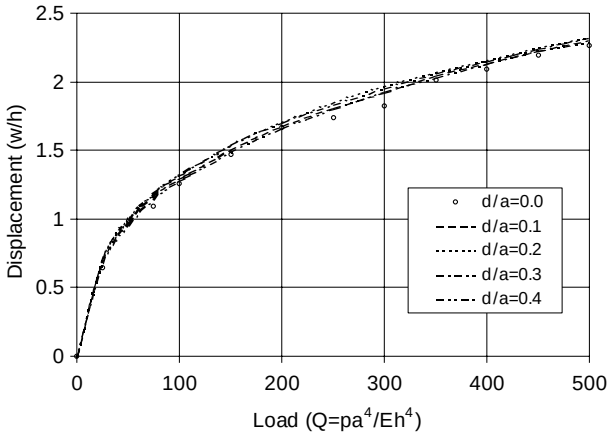

Fig. 6. Pinned square plate with free circular hole.

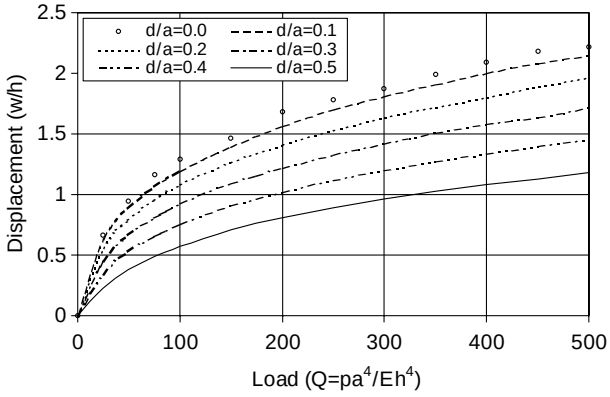

Fig. 7. Pinned square plate with guided circular hole.

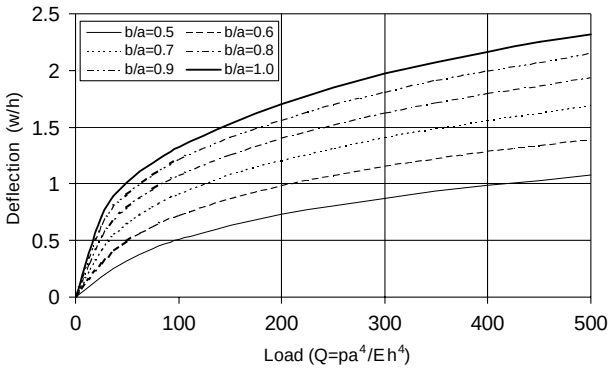

Fig. 8. Pinned rectangular plate with free circular hole ($d/a = 0.2$).

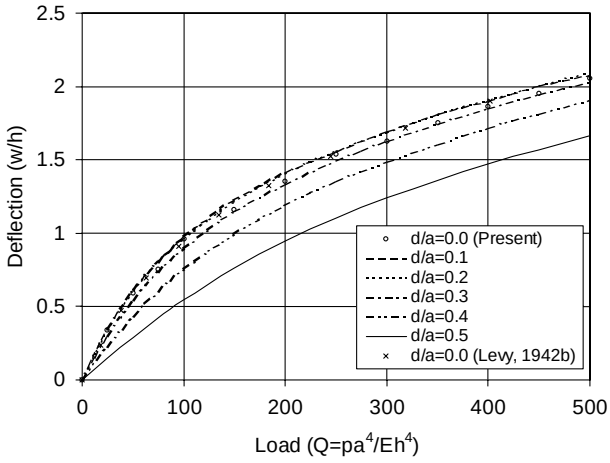

Fig. 9. Fixed square plate with free circular hole.

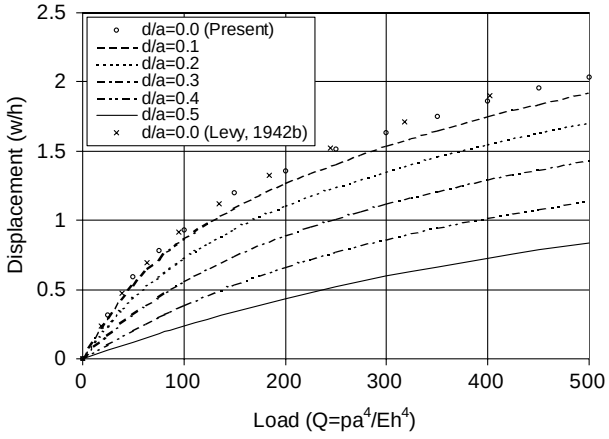

Fig. 10. Fixed square plate with guided circular hole.

Case 2. Annular circular plate. Annular circular plate subjected to uniformly distributed transverse load is also analysed by considering four segments in the model as shown in Fig. 4. The inside and outside diameters of the plate are denoted by d and a respectively. The conditions at the inside edge and the symmetry axes are the same as those as described earlier for the rectangular plate with a circular opening.

Results for the pinned outside edge are presented in Figs. 11 and 12, where the first corresponds to the case having no restraint at the hole and the second with in-plane restraint. When the inside hole is free, results do not converge properly if d/a is larger than 0.3 and the curve behaves erratically beyond $Q = 200$ (Fig. 11). When the in-plane movement of the inside boundary is restrained, convergence is achieved for cases with d/a being 0.4 and 0.5. The curves are also separated with higher deflections for lower values of d/a. Results for the clamped circular plate with inside edge free and guided are shown in Figs. 13 and 14

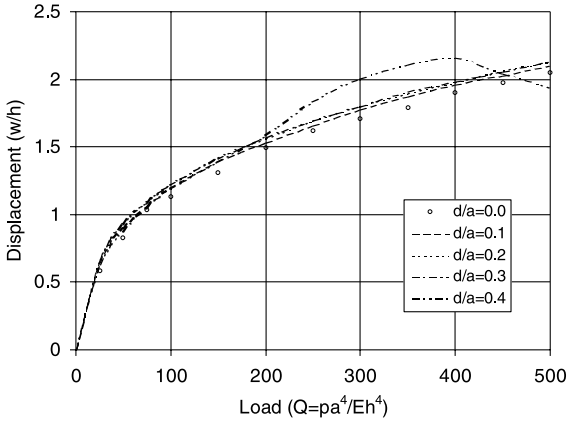

Fig. 11. Pinned circular plate with free circular hole.

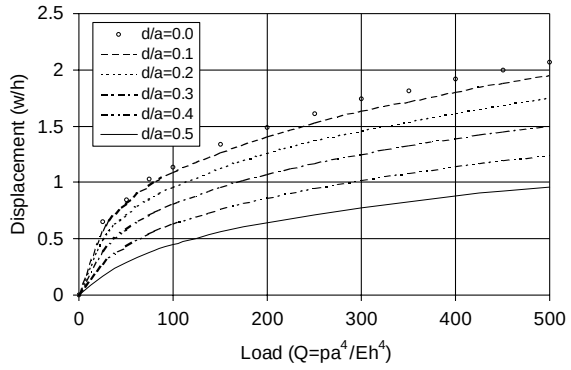

Fig. 12. Pinned circular plate with guided circular hole.

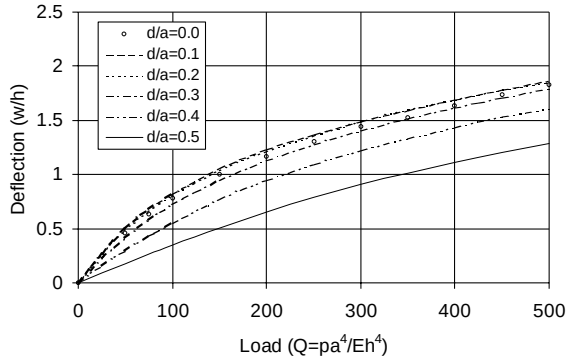

Fig. 13. Fixed circular plate with free circular hole.

respectively. In these cases, results converge with number of iterations, deflection increases monotonically with the load and small deflection is found for large size hole.

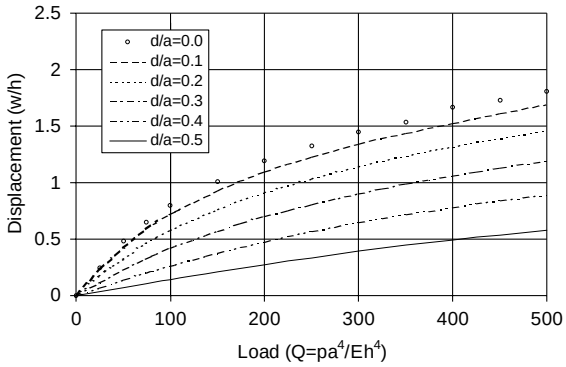

Fig. 14. Fixed circular plate with guided circular hole.

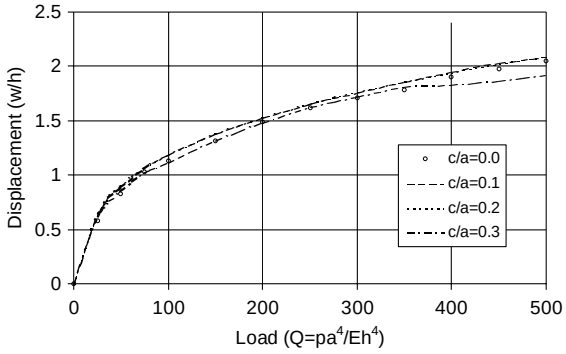

Fig. 15. Pinned circular plate with free square hole.

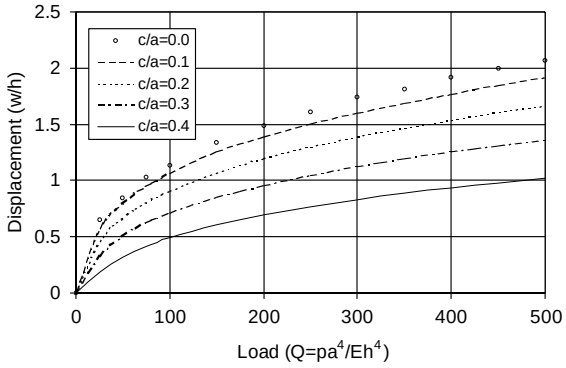

Fig. 16. Pinned circular plate with guided square hole.

Case 3. Circular plate with a square opening. Results for the circular plate with a square opening are presented in Figs. 15–18 with the same combinations of boundary conditions discussed above. The response of this plate is very similar to those of the circular annular plate.

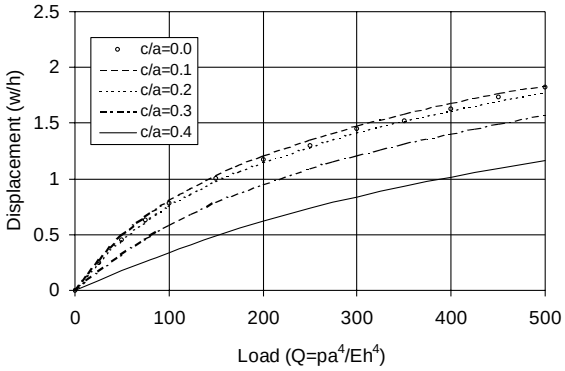

Fig. 17. Fixed circular plate with free square hole.

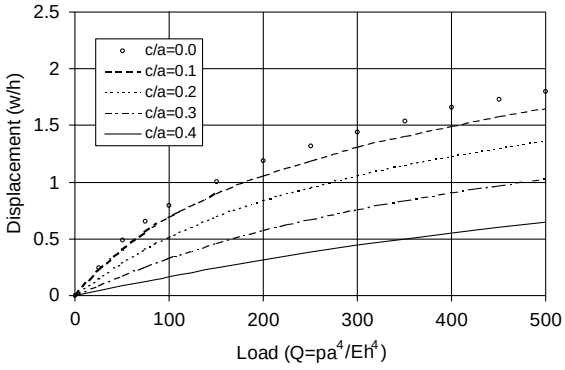

Fig. 18. Fixed circular plate with guided square hole.

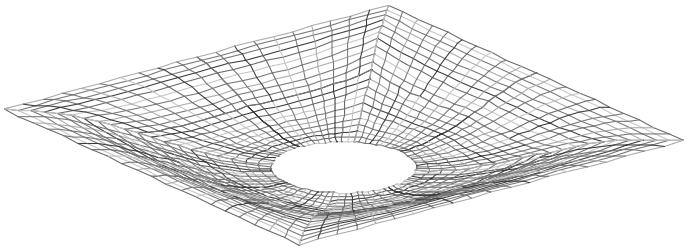

Fig. 19. Clamped square plate with guided circular hole: $Q = 500$, $d/a = 0.3$.

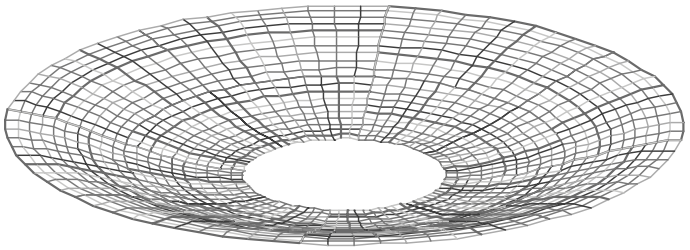

Fig. 20. Clamped circular annular plate with guided hole: $Q = 500$, $d/a = 0.3$.

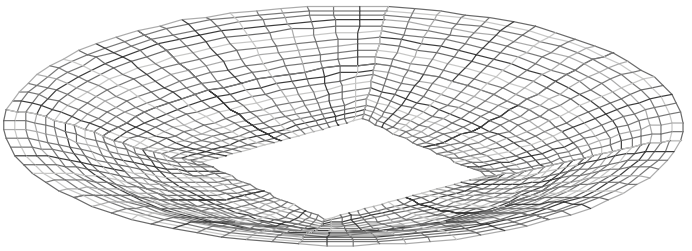

Fig. 21. Clamped circular plate with guided square hole: $Q = 500$, $c/a = 0.3$.

The deflected shapes for the above three cases are shown in Figs. 19–21. The load parameter used for these plots is 500 and the ratio of hole size (d or c) to the outer physical length (a) considered is 0.3.

6. Concluding remarks

A modified version of the Ritz method has been used for the geometrically nonlinear static analysis of elastic rectangular and circular plates with openings. Each plate model consists of four quadrilateral segments, which are then assigned two types of nodal points. The first type consists of eight nodes that define the geometry of the segment. Using the second type, components of the displacement and rotation of the normal to the middle surface of the plate are interpolated by much higher order polynomial than the one used for the geometry. The deflection for a given load is obtained iteratively and increases monotonically with the load. For the higher load parameter, the convergence is somewhat slow. When the opening size is in the neighbourhood of 40–50% of the overall size of the plate, results do not converge properly if there is no constraint on the opening. But when the opening is constrained against in-plane movement, results converge even for large openings.

The formulation used in the present analysis has many advantages over the finite element method, such that only a few segments can be used in the analysis of plates having complex geometry. In some finite element formulations, term in the interpolating function is dropped depending on the number of nodal points chosen for the element. This can cause inconsistency in the displacement field and be a source of error. The interpolation function used for the displacement and rotation parameters in the present formulation is complete.

References

Bergan, P.G., Clough, R.W., 1973. Large deflection analysis of plates and shallow shells using finite element method. Int. J. Numer. Methods Engng. 5, 543.

Berger, H.M., 1955. A new approach to the analysis of large deflections of plates. ASME J. Appl. Mech. 22, 465–472.

Courant, R., 1943. Variational methods for the solution of problems of equilibrium and vibrations. Bull. Am. Math. Soc. 49, 1–23.

Higgins, T.J., 1943. The approximate mathematical methods of applied physics as exemplified by application to Saint-Venant's torsion problem. J. Appl. Phys. 14, 469–480.

Leissa, A.W., 1969. Vibration of plates, NASA SP-160.

Leissa, A.W., 1973. The free vibration of rectangular plates. J. Sound Vib. 31, 257–293.

Levy, S., 1942a. Bending of rectangular plates with large deflections, NACA TR 737.

Levy, S., 1942b. Square plate with clamped edges under normal pressure producing large deflections, NACA TR 740.

Murray, D.W., Wilson, E.L., 1969. Finite element large deflection analysis of plates. ASCE J. Engng. Mech. Div. 95, 143–165.

Novozhilov, V.V., 1953. Foundations of the Nonlinear Theory of Elasticity. Graylock Press, Rochester, NY.

Pica, A., Wood, R.D., Hinton, E., 1980. Finite element analysis of geometrically nonlinear plate behaviour using a Mindlin formulation. Comput. Struct. 11, 203–215.

Pickett, G., 1939. Solution of rectangular clamped plate with lateral load by generalized Energy method. ASME J. Appl. Mech. 6, A-168–A-170.

Rushton, K.R., 1970. Large deflexion of plates with initial curvature. Int. J. Mech. Sci. 12, 1037–1051.

Satyamoorthy, M., 1997. Nonlinear Analysis of Structures, second ed. CRC Press, Boca Raton.

Singh, A.V., Elaghabash, Y., 2003. On the finite displacement analysis of quadrangular plates. Int. J. Nonlinear Mech. 38, 1149–1162.

Timoshenko, S., 1934. Theory of Elasticity. McGraw-Hill Book Company, New York.

Wang, C.-T., 1948. Bending of rectangular plates with large deflections, NACA TN 1462.

Warburton, G.B., 1954. The vibration of rectangular plates. Proc. Inst. Mech. Engineers, Ser. A 168, 371–384.

Weaver Jr., W., Johnston, P.R., 1984. Finite Elements for Structural Analysis. Prentice-Hall, Englewood Cliffs, NJ.

Yang, T.Y., 1972. Finite displacement plate flexure by the use of matrix incremental method. Int. J. Numer. Methods Engng. 4, 415–432.

Young, D., 1950. Vibration of rectangular plates by the Ritz method. ASME J. Appl. Mech. 17, 448–453.